ORIGINAL RESEARCH

Exosome-Loaded GelMA Hydrogel as a Cell-Free Therapeutic Strategy for Hypertrophic Scar Inhibition

Hui Wang[1,2], Xijuan Gao[2], Yanxia Zhao[2], Shudong Sun[2], Yuxiu Liu [ID][1], Kun Wang[2]

[1]School of Nursing, Shandong Second Medical University, Weifang, People's Republic of China; [2]Department of Burns and Wound Repair, Weifang People's Hospital, Shandong Second Medical University, Weifang, People's Republic of China

Correspondence: Yuxiu Liu, School of Nursing, Shandong Second Medical University, Weifang, People's Republic of China, Email 18663608162@163.com; Kun Wang, Department of Burns and Wound Repair, Weifang People's Hospital, Shandong Second Medical University, Weifang, People's Republic of China, Email wangkun8192165@126.com

Purpose: Hypertrophic scar (HS) is a fibrotic proliferative disorder that arises from an abnormal wound healing process. It is a significant clinical challenge, primarily characterized by the excessive accumulation of extracellular matrix (ECM) and abnormal angiogenesis. This study introduces a novel injectable hydrogel system that integrates sustained-release Exosomes for targeted hypertrophic scar modulation. Exosomes (Exos) from adipose-derived stem cells (ASCs) are emerging as promising treatment for hypertrophic scar inhibition. But when treated independently, it must be applied regularly multiple times to maintain its optimal concentration. Gelatin Methacryloyl (GelMA) hydrogel is an ideal biomaterial candidate for engineering skin tissues because of its similarity to ECM, and importantly GelMA hydrogel can maintain drug concentrations via the encapsulation and sustained release of it, which enhances the potential of clinical applications.

Methods: The Exosome-Loaded GelMA Hydrogel (Exos-GelMA) hydrogel was fabricated and characterized for its pore size and biocompatibility. A rabbit ear HS model was established. Three skin defects on each ear were treated with GelMA hydrogel, Exos-GelMA hydrogel, or left untreated as a blank group. The effects of HS inhibition were assessed through Hematoxylin and Eosin (HE) staining, Masson's trichrome staining, and immunohistochemical staining of Collagen I (COL I), Collagen III (COL III), α-smooth muscle actin (α-SMA), as well as immunofluorescence staining of vascular endothelial growth factor (VEGF).

Results: The Exos-GelMA hydrogel demonstrated an appropriate pore size distribution, excellent biocompatibility, and enhanced fibroblast proliferation in vitro. In the rabbit ear HS model, the Exos-GelMA hydrogel significantly inhibited excessive collagen fiber deposition and the overexpression of the angiogenic factor VEGF. Quantitative analysis of immunohistochemical and immunofluorescence staining showed comparing to blank group the Exos-GelMA hydrogel significantly reduced COL I deposition by 43%, COL III deposition by 15%, α-SMA expression by 31%, and VEGF expression by 35% at 28 day.

Conclusion: In summary, the Exos-GelMA composite hydrogel exhibits significant potential for the prevention and treatment of HS. This study supports the feasibility of Exos-GelMA as a cell-free therapeutic approach for the management of HS.

Keywords: hypertrophic scar, ADSC-exosomes, GelMA hydrogel, collagen, angiogenesis, cell-free therapy

Introduction

Skin tissue damage is a common pathological condition encountered in clinical diagnosis and treatment, with abnormal healing processes frequently leading to the formation of pathological scars. HS, a typical example of fibrotic diseases, is characterized by persistent inflammatory responses and abnormal deposition of extracellular matrix (ECM).[1–3] Epidemiological data indicate that the overall incidence of HS ranges from 4% to 16%, with the incidence in post-surgical burn patients reaching as high as 70%. Current common therapies including gel sheets, tape fixation, topical and injected external agents, laser treatment, radiation therapy, and oral agent therapy should be administered on a case-by-case basis. At present, there is no singular treatment method that consistently achieves satisfactory results for HS. The combined application of various treatment methods can achieve an effectiveness rate of over 90%, while the efficacy of

single treatments tends to be more moderate. Therefore, a comprehensive treatment approach remains the preferred clinical option. In addition, there are also certain side effects. For example, studies have shown that patients injected with triamcinolone experienced significant improvements in the thickness and appearance of scars, but 15% of patients reported side effects like skin atrophy and pigmentation changes.[4–6] HS not only impair physiological functions, such as skin barrier integrity and joint mobility, but also negatively impact patients' psychological well-being due to their conspicuous deformities, resulting in a dual burden of physiological and psychological distress.[7,8] Early management and intervention of scars can help shorten the immature phase and improve overall scar outcomes. Therefore, the development of effective early intervention strategies is of significant clinical importance.

The process of skin wound healing encompasses four dynamic phases: hemostasis, inflammation, proliferation, and remodeling.[9] During normal physiological healing, dermal fibroblasts, regulated by cytokines such as transforming growth factor-beta (TGF-β), play a crucial role in tissue repair by secreting COL I and COL III, as well as α-SMA, ultimately achieving a balanced ECM. However, in the formation of HS, the sustained activation of pathological myofibroblasts results in an imbalance between collagen synthesis and degradation, with their excessive contractile properties further contributing to scar contraction. Molecular pathological studies have indicated that the aberrant activation of the TGF-β/Smad signaling pathway is a fundamental mechanism driving excessive ECM deposition, thereby providing a theoretical basis for targeted interventions.[10–12]

Mesenchymal stem cells (MSCs) are essential cellular components in regenerative medicine, with their paracrine mechanisms playing a pivotal role in tissue repair. Recent studies have shown that exosomes derived from MSCs (MSCs-exosomes, MSCs-exos), which are nanoscale vesicles measuring between 30 to 150 nm in diameter, not only transport bioactive molecules but also facilitate wound healing through mechanisms that regulate fibroblast-to-myofibroblast transdifferentiation and modulate the immune microenvironment. In comparison to primary MSCs, MSCs-exos offer the dual advantages of low immunogenicity and no tumorigenic risk (lack of nuclear structures), making them an ideal candidate for Cell-free therapies.[13–15]

Adipose-derived stem cells (ADSCs) have emerged as a significant source for exosome research due to their ease of acquisition and robust proliferation capabilities. ADSC-derived exosomes (ADSC-Exos) can significantly modulate the collagen metabolic balance within the wound microenvironment, achieving scar inhibition by downregulating pro-fibrotic factors and upregulating anti-fibrotic factors.[16,17] ADSC-Exos contain NcRNAs such as MicroRNAs (MiRNAs), Long non-coding RNAs (LncRNAs), Circular RNAs (circRNAs), and proteins that suppress fibrosis.[14] For instance, ADSC-Exos inhibited skin fibrosis by regulating miR-128-1-5p/TGF-β1/Smad signaling pathway in diabetic wound healing[18] and reduced scar formation and lowering pro-inflammatory and fibrotic indicators through miR-194 modulation.[19] However, the rapid metabolism of free exosomes limits their therapeutic efficacy, prompting current research to adopt biomaterial loading strategies to extend their duration of action.

Hydrogel materials are characterized by their three-dimensional porous structure and properties that mimic ECM and offer distinct advantages in drug delivery systems. Natural hydrogels, such as alginate, chitosan, and hyaluronic acid, exhibit excellent biocompatibility. However, they possess relatively poor mechanical properties and high expansion rates, which limit their applications across various fields. Through chemical modification or by combining them with synthetic materials, it is possible to enhance the mechanical properties of synthetic hydrogels while retaining the biocompatibility and bioactivity of natural hydrogels. In this study, we employed GelMA hydrogel, which is a chemically modified natural material and synthesized through photopolymerization techniques to create scaffolds with controllable degradation rates. The molecular network of GelMA effectively encapsulates ADSCs-Exos and maintains a locally effective concentration at the wound site through a sustained release mechanism. Preliminary studies have confirmed that the mechanical properties of GelMA demonstrate favorable biomechanical compatibility with natural skin tissue, thereby providing an appropriate microenvironment for ECM reconstruction.[20,21] In addition, currently there are already hydrogel products (such as GelrinC®) approved for market release abroad. GelMA hydrogel, being the most widely and deeply studied hydrogel, is considered to have the potential for clinical translation.

This study innovatively constructs an injectable GelMA composite hydrogel loaded with ADSCs-Exos (Exos-GelMA) and systematically evaluates its effects on HS. The experimental design includes: (1) assessing biocompatibility using the CCK-8 assay; (2) establishing a rabbit ear hypertrophic scar model to dynamically observe the wound healing

process; (3) employing multimodal histological analysis techniques, including hematoxylin and eosin (HE) staining and Masson's trichrome staining, to quantitatively evaluate collagen deposition; and (4) utilizing immunohistochemistry and immunofluorescence staining to detect the expression of key factors such as COL I, COL III, α-SMA, and VEGF. The results of this study will provide new theoretical foundations and technical pathways for acellular therapeutic strategies based on exosomes and hydrogels.

Materials and Methods

Preparation of Exos-GelMA

GelMA hydrogels and lithium phenyl-2,4,6-trimethylbenzoylphosphinate (LAP) photoinitiator were obtained from Shanghai Huaxiasiyin Biotechnology Co., Ltd. Exosomes were derived from ADSCs were supplied by Cyagen Biosciences Inc and handled under aseptic conditions. Following established protocols,[22] 10% (w/v) GelMA was dissolved in phosphate-buffered saline (PBS, Gibco, USA) and placed in a water bath at 50°C for complete dissolution. This solution was then uniformly mixed with 0.2% (w/v) LAP. The resulting mixture was filtered through a 0.22 μm sterile filter and supplemented with ADSCs-Exos to achieve a final concentration of 100 μg/mL. The Exos-GelMA composite hydrogel was stored in the dark at 4 °C for future use.

Morphological Characterization

After ultra-violet (UV) irradiation (365nm, 20mW/cm2) for 5 s, the gel formation characteristics were observed using a digital single-lens reflex camera (Nikon, Tokyo, Japan). Following freeze-drying and gold sputter coating, the Exos-GelMA hydrogel was imaged using a scanning electron microscope (SEM, Philips XL-30, Amsterdam, Netherlands) at an acceleration voltage of 15 kV. The pore size distribution of the hydrogel was quantitatively analyzed based on SEM images using ImageJ software.

Cell Culture

Healthy New Zealand White rabbits were anesthetized with 3% pentobarbital sodium (30 mg/kg), and ear skin tissue was collected under sterile conditions. The tissue samples were thoroughly rinsed with PBS and placed in Dulbecco's Modified Eagle Medium (DMEM, Gibco, USA) containing 0.2 mg/mL dispase II for 2 hours at 37°C to facilitate digestion. The epidermal and dermal layers were separated using mechanical methods. The dermal tissue was cut into fragments smaller than 5 mm^3 and digested with trypsin (Gibco, USA) at 37°C for 10 minutes. Following centrifugation at 150×g for 10 minutes, the cells were collected and resuspended in DMEM/Ham's F12 culture medium supplemented with 10% fetal bovine serum (FBS, Gibco) and 1% penicillin-streptomycin (Gibco, USA). The cells were then cultured in a 37°C incubator with 5% CO_2 for expansion.[23] Fibroblasts at passage two (P2) were used for subsequent experiments.

Cell Viability Assay

GelMA and Exos-GelMA were immersed in DMEM culture medium (material surface area/extraction liquid volume = 3 cm²/mL) for 72 hours to obtain the extraction solution. P2 fibroblasts were seeded at a density of 2×10^3 cells per well in a 96-well plate. CCK-8 reagent (Dojindo, Kumamoto, Japan) was added at 1, 3, and 5 days post-seeding, and the absorbance was measured at 450 nm using a microplate reader (Multiskan FC, Thermo Fisher, USA) to calculate cell viability, thereby assessing the biocompatibility of the materials.

Establishment of Rabbit Ear Scar Model

The experimental protocol was approved by the Animal Ethics Committee of Weifang People's Hospital and strictly adhered to Chinese Regulations on the Management of Experimental Animals. Nine male New Zealand rabbits aged three months (weighing 2.5 ± 0.3 kg) were obtained from Qingdao Kangdaaibo Biotechnology Co., Ltd. The rabbits were acclimatized under standard husbandry conditions for one week. Three full-thickness skin defects were created on rabbit each ear, which measuring 10 mm in diameter and extending to the cartilaginous membrane.[24] The three skin defects on each ear were randomly assigned to three groups: a blank group (untreated), a GelMA group, and an Exos-GelMA group.

During treatment, GelMA and Exos-GelMA hydrogels were applied to the wounds, followed by in situ curing using 365 nm ultraviolet light (20 mW/cm²) for 5 seconds. Tissue samples were collected for analysis at 14, 28 days post-surgery.

Histological and Immunohistochemical Staining Analyses

The tissue samples were fixed in 4% paraformaldehyde for 24 hours, followed by dehydration through a graded series of ethanol and embedding in paraffin. Serial sections with a thickness of 5 μm were prepared for subsequent analyses. HE staining and Masson's trichrome staining were employed to evaluate cellular and tissue morphology, collagen distribution. Additionally, immunohistochemical staining was performed to assess the expression levels of COL I, COL III, α-SMA, and VEGF. The quantitative analysis of Immunohistochemistry and immunofluorescence staining was conducted utilizing ImageJ software. Blinding during the analysis of research data.

Scar Elevation Index (SEI)

SEI is a widely utilized metric for scar assessment and directly proportional to scar thickness. The SEI was calculated from the images of HE staining using the following formula:

$$SEI = \frac{H_1}{H_2}$$

Where H_1 represents the vertical distance from the highest point of the scar to the surface of the ear cartilage, H_2 represents the vertical distance from the surrounding normal skin to the surface of the ear cartilage.[25] The mean value was obtained from three sections for each sample.

Statistical Analysis

Statistical analysis was conducted using SPSS 26.0, with data presented as mean ± standard deviation. A one-way ANOVA was employed to assess statistical significance, with p-values less than 0.05 considered statistically significant. Use Tukey's HSD method for post-hoc correction of ANOVA. (*$p < 0.05$, **$p < 0.01$, ***$p < 0.001$, ****$p < 0.0001$).

Results

Characterization of Exos-GelMA

Dressings suitable for wound repair must demonstrate excellent biocompatibility, appropriate pore size, porosity, mechanical properties, and degradation rate. In this study, we selected a GelMA hydrogel prepared at a concentration of 10% (w/v), which has been reported in the literature to possess mechanical properties comparable to those of skin and a degradation rate similar to that of wound healing.[26] Following the exposure to ultraviolet light for 5 seconds, it was observed that the Exos-GelMA hydrogel gelled well. (Figure 1A) SEM images revealed that after freeze-drying the Exos-GelMA hydrogel exhibited highly interconnected and continuous micropores with a uniform distribution. (Figure 1B) Analysis using ImageJ software indicated an average pore size of (133.63 ± 27.31) μm. (Figure 1C) The pore architecture of three-dimensional polymeric scaffolds is recognized as a fundamental factor in tissue engineering, as it establishes the essential framework for the seeded cells to develop into functional tissue. The design of the scaffold significantly influences cell growth and proliferation. As previous reported, pore sizes less than 160 μm, were optimal for the adhesion and growth of human skin fibroblast.[27–31] Hence, the pore size of (133.63 ± 27.31) μm was conducive to cell growth and proliferation within the material.

Subsequently, the CCK-8 assay was utilized to evaluate the effects of Exos-GelMA hydrogel on the viability and proliferation of fibroblasts, with the aim of assessing the safety of GelMA hydrogel and the proliferative capacity of ADSCs-Exos. The absorbance results obtained on days 1, 3, and 5 indicated that cell viability in the GelMA hydrogel group was nearly identical to that of the blank group, suggesting that the hydrogel does not adversely affect cell survival. Importantly, cell proliferation in the Exos-GelMA hydrogel group was significantly higher than in the other two groups, indicating that ADSCs-Exos have the capacity to promote the proliferation of rabbit fibroblasts. (Figure 1D) In conclusion, the combination of ADSCs-Exos and GelMA hydrogel represents a promising strategy for effectively loading cells and enhancing cell proliferation.
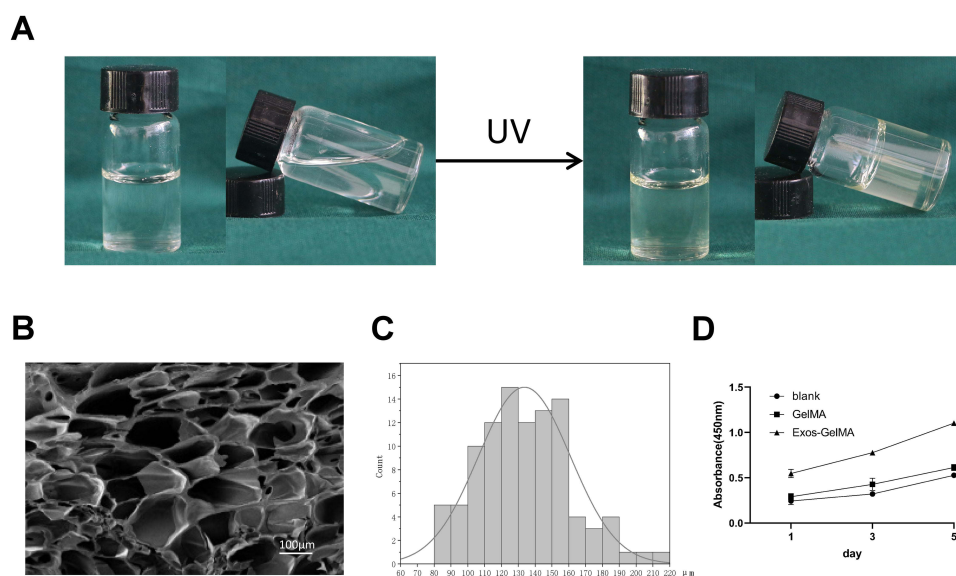
Figure 1 Characterization of Exos-GelMA hydrogel. Exos-GelMA hydrogel under UV irradiation (**A**) before and (**B**) after. (**C**) SEM images of Exos-GelMA hydrogel. (**C**) Pore size distribution of Exos-GelMA hydrogel. (**D**) CCK-8 assay of blank, GelMA, and Exos-GelMA hydrogel group.

## In vivo Wound Healing and Evaluation of Hypertrophic Scar

To further validate the efficacy of the early application of Exos-GelMA hydrogel in mitigating HS and promoting wound healing, we conducted in vivo experiments. Gross observation revealed that both the GelMA and Exos-GelMA groups demonstrated superior wound healing compared to the blank group on postoperative day 14, with the Exos-GelMA group achieving an 80% wound closure rate. By day 28, all groups exhibited complete wound closure; however, the blank and GelMA groups displayed prominent scar characteristics, including raised, contracted, erythematous, and palpable scars indicative of HS. In contrast, the Exos-GelMA group exhibited flatter, less contracted scars with reduced erythema. (Figure 2A and B)

Histological analysis of wound sections was performed using HE and Masson's trichrome staining to assess cellular organization, tissue architecture, and collagen deposition. The Exos-GelMA group demonstrated well-organized, parallel-aligned collagen fibers, minimal neovascularization, and reduced inflammatory responses. In contrast, the blank and GelMA groups exhibited disorganized collagen bundles, excessive collagen accumulation, significant inflammation, and pronounced neovascularization. (Figure 3A–D)

A quantitative measure of the SEI was significantly lower in the Exos-GelMA group (1.27 ± 0.03) compared to the GelMA (2.60 ± 0.04) and control (3.95 ± 0.06) groups at day 28. (Figure 3) These findings suggest that the Exos-GelMA hydrogel effectively reduces scar hypertrophy and promotes regenerative healing. (Figure 3E and F)

Exos-GelMA Suppresses Excessive ECM Deposition and Angiogenesis

Scar tissue is characterized by excessive deposition of collagen fibers. COL I and COL III are major components of the ECM and are both upregulated during scar formation. α-SMA was a critical mediator of myofibroblast contraction, scar contracture, and hyperactive wound healing and reflects the cellular specialization that occurs during the differentiation of fibroblasts into myofibroblasts.[32,33] Immunohistochemical results revealed that compared to the blank and GelMA hydrogel groups, the Exos-GelMA hydrogel group exhibited reduced expression of COL I on the 14th and 28th day. However, the expression of COL III varies among the three groups. On day 14, the deposition of COL III in the blank group was much greater than in the GelMA and Exos-GelMA hydrogel group, while the Exos-GelMA group was slightly higher than the GelMA group. By day 28, the deposition of COL III in the Exos-GelMA group was significantly lower
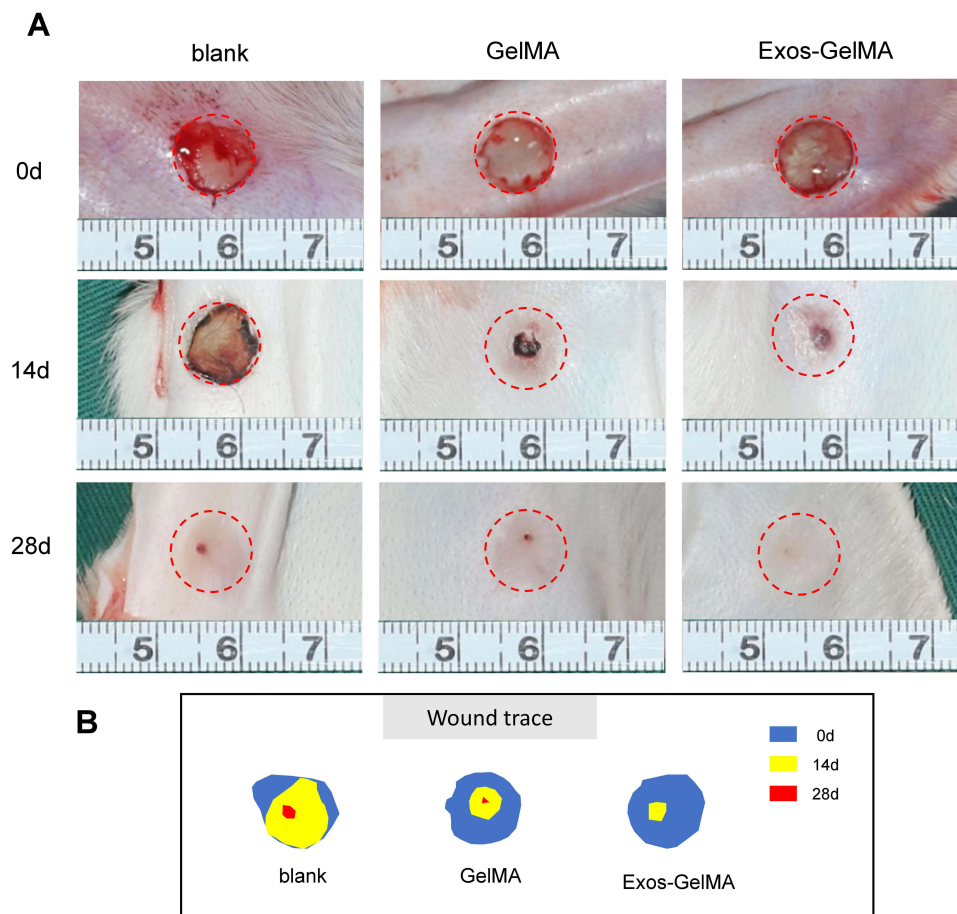
Figure 2 In vivo wound healing. (**A**) Gross view, (**B**) wound trance of wounds treated with GelMA and Exos-GelMA hydrogel at 0, 14, and 28 days. The Red outlines were the area of skin defects as scar model.

than in the other two groups. (Figure 4A and B) Quantitative analysis of immunohistochemical staining of COL showed comparing to blank group the Exos-GelMA hydrogel significantly reduced COL I deposition by 43%, and COL III deposition by 15% on the 28th day. (Figure 5A and B) The immunohistochemical staining of α-SMA showed that on the 14th day α-SMA expression in blank and Exos-GelMA group obviously lower than GelMA group; on the 28th day α-SMA expression in blank group was on the rise and Exos-GelMA hydrogel inhibit α-SMA expression that made it have little change. (Figure 4C) Quantitative analysis of immunohistochemical staining of α-SMA showed com-paring to blank group the Exos-GelMA hydrogel reduced by 31% on the 28th day. (Figure 5C)

VEGF-mediated neovascularization plays a crucial role in the pathogenesis of HS. Newly formed blood vessels supply oxygen and nutrients to scar tissue while secreting pro-fibrotic factors (eg, TGF-β1, PDGF), thereby further stimulates the differentiation of fibroblasts into myofibroblasts and accelerates collagen deposition.[3,34] In this study, immunofluorescence staining for VEGF revealed significantly lower expression levels in the Exos-GelMA hydrogel group compared to the blank and GelMA groups. (Figure 4D) Quantitative analysis of immunofluorescence staining of VEGF showed comparing to blank group the Exos-GelMA hydrogel significantly reduced VEGF expression by 35% at 28 day. (Figure 5D)

In conclusion, the Exos-GelMA hydrogel enhances the organization of the ECM architecture and mitigates patholo-gical vascular hyperplasia, highlighting its therapeutic potential in regulating scar progression.
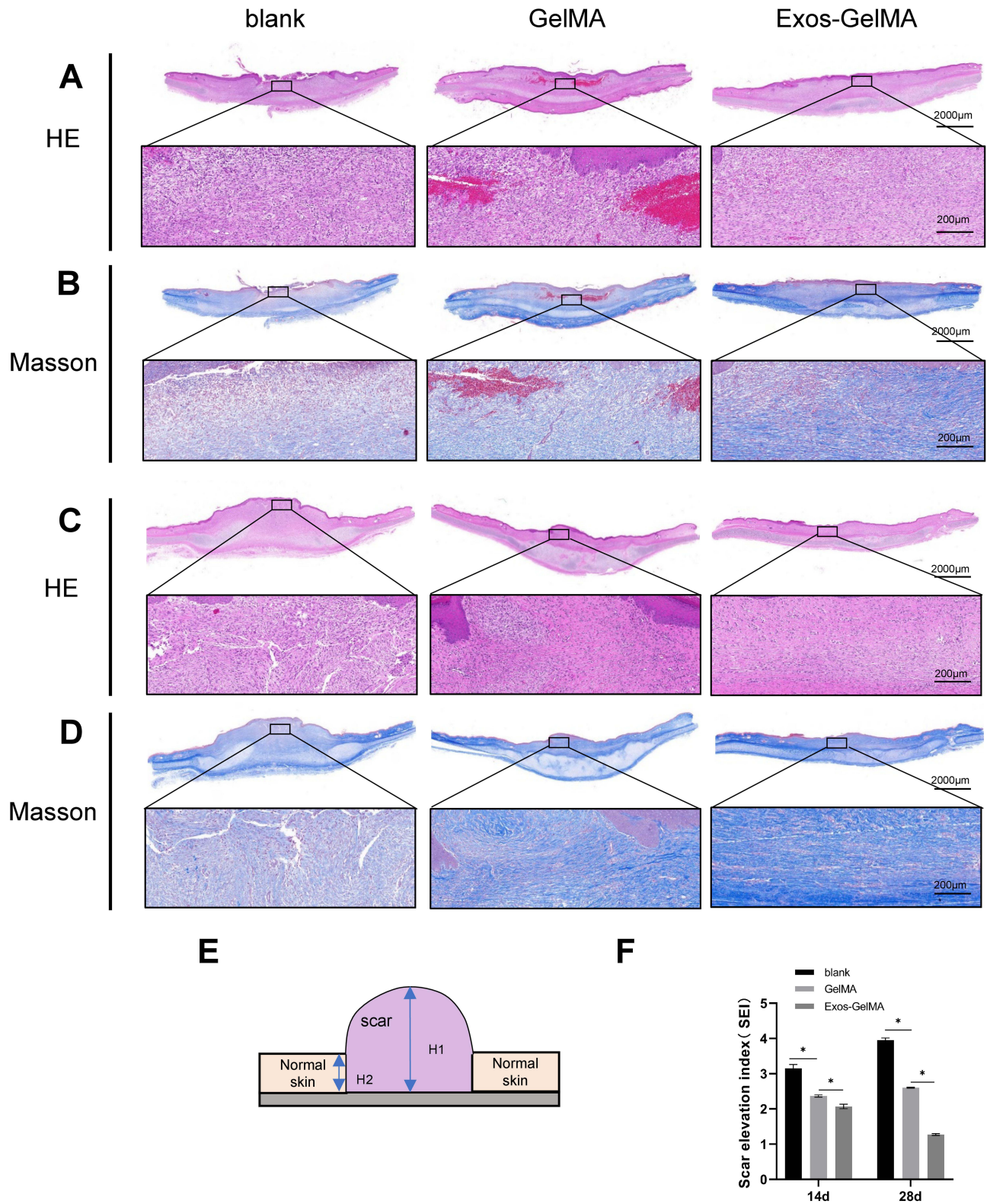
Figure 3 Histological staining. (**A**) HE and (**B**) Masson staining of wound at 14 days. (**C**) HE and (**D**) Masson staining of wound site at 28 days. (**E**) Diagram of scar elevation index calculation (SEI). (**F**) SEI assay calculated from HE staining. (*P<0.05).
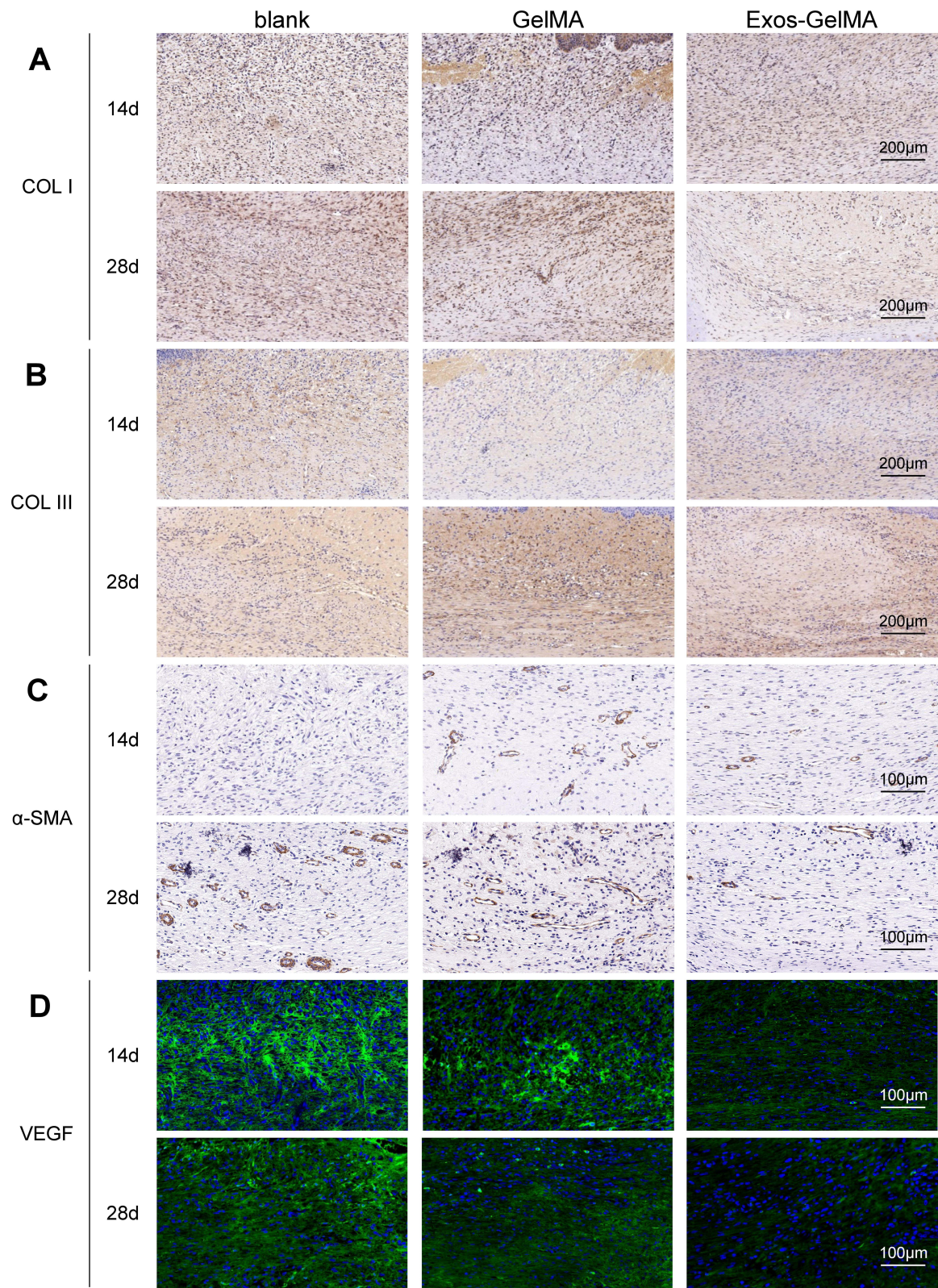
Figure 4 Immunohistochemical and Immunofluorescence staining. Immunohistochemical staining of (**A**) COL I, (**B**) COL III, and (**C**) α-SMA. Immunofluorescence staining of (**D**) VEGF.
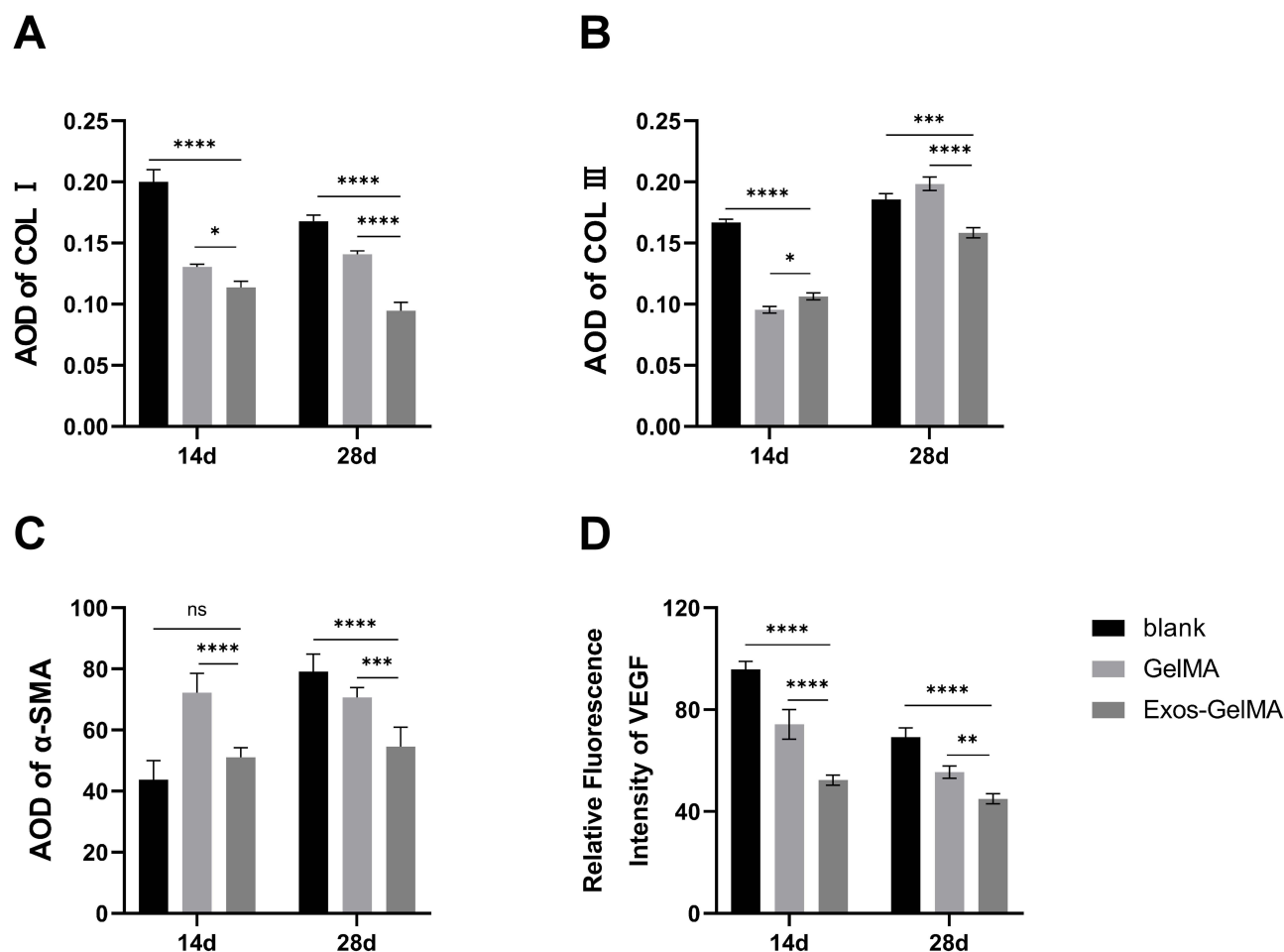
Figure 5 Quantitative analysis of immunohistochemical and immunofluorescence staining. Quantitative analysis of (**A**) COL I, (**B**) COL III, (**C**) α-SMA, and (**D**) VEGF. (*$p < 0.05$, **$p < 0.01$, ***$p < 0.001$, ****$p < 0.0001$).

Discussion

HS are a common consequence of pathological wound healing, presenting dual challenges in clinical management. On one hand, scar contraction leads to significant skin dysfunction, which greatly diminishes patients' quality of life. On the other hand, the abnormal aesthetic appearance of these scars induces psychosocial stress, further exacerbating the overall disease burden. Current clinical intervention strategies including corticosteroid injections, 5-fluorouracil, radiation therapy, and laser therapy can partially alleviate symptoms. However, their efficacy is uncertain with effectiveness rates ranging from 30% to 70%. Additionally, these treatments may result in potential side effects, such as skin atrophy and pigment loss, and no standardized treatment protocol has been established.[35,36] Consequently, developing preventive treatment methods that target the pathological mechanisms underlying HS formation remains a critical research focus in the field of regenerative medicine. There is an urgent need to create new intervention strategies that are both preventive and therapeutic.

This study is based on the concept of "mechanical-biological coupling regulation" and innovatively develops a GelMA composite hydrogel system loaded with ADSC-Exos. The objective is to impede key pathological processes involved in HS formation through multimodal intervention. Material characterization results indicate that the three-dimensional interpenetrating network structure of GelMA not only accurately simulates the topological features of the natural ECM but also modulates fibroblast behavior through mechanical signal transduction mechanisms, due to its photo-crosslinking properties. The mechanical properties of the scaffold material can influence cytoskeletal reorganization via the integrin-focal adhesion pathway, thereby inhibiting pathological ECM deposition.[37–39] Notably, following the

incorporation of ADSC-Exos, the proliferation activity of fibroblasts in the Exos-GelMA group was significantly enhanced compared to the blank group, confirming that the bioactive molecules carried by ADSC-Exos can synergistically augment the material's pro-repair functions.

The remodeling stage of wound healing is a critical period for scar formation. During this stage, the excess ECM is primarily degraded by proteolytic enzymes to maintain a dynamic balance between collagen synthesis and degradation. When this balance is disrupted, with a significant increase in COL I synthesis and a decrease in degradation, it leads to excessive collagen deposition, which is the primary cause of HS formation.[40,41] The abnormal activation of fibroblasts into myofibroblasts is the main factor contributing to this imbalance, a process stimulated by growth factors such as TGF-β and platelet-derived growth factor. These myofibroblasts exhibit enhanced synthetic capacity, significantly promoting the excessive deposition of COL I in HS and exacerbating scar fibrosis.[42,43] Studies have demonstrated that high-concentration ADSC-Exos not only reduce collagen formation but also enhance the structural arrangement of collagen, making it more organized. Additionally, ADSC-Exos promote the migration and proliferation of fibroblasts, which is advantageous for wound healing. As ADSC-Exos downregulate the expression of α-SMA in fibroblasts, this suggests an increased rate of fibroblast migration from the periphery to the wound center, thereby reducing surface tension and inhibiting the excessive formation of HS.[18,19,44] In this study, the Exos-GelMA composite hydrogel not only inhibits the excessive deposition of COL I and COL III but also promotes a more orderly arrangement of collagen fibers. Although the expression of α-SMA has decreased, the difference has not yet reached statistical significance.

Excessive angiogenesis is a significant component of the pathophysiology of HS.[45,46] In scar tissue, fibroblasts are closely associated with blood vessels and communicate through the transport of nutrients and signal transduction. Blood vessels deliver oxygen and nutrients to fibroblasts via endothelial channels, creating a microenvironment that promotes the survival and proliferation of these cells. As effector cells regulated by their microenvironment, fibroblasts secrete collagen to form scars. Consequently, blood vessels and collagen serve as upstream and downstream factors of fibroblast activity, respectively.[47–53] Based on this understanding, we hypothesize that inhibiting excessive angiogenesis can effectively control the overproliferation of fibroblasts, thereby reducing the excessive production of collagen. At present, interventions aimed at the vascular system, including intense pulsed light therapy, pulsed dye lasers, vascular endothelial growth factor antibodies, and Endostar, have become potential therapeutic options.[47] Extensive research has indicated that ADSCs and their Exo possess the capability to inhibit the formation of hypertrophic scar.[13,18,40,54–59] Among them, VEGF serves as a critical regulator in the process of vascular regeneration. Xu et al [19] provided strong evidence that VEGF expression was decreased treated with miR-194 of ADSC-Exos. Similarly, the findings of this study further corroborate the aforementioned conclusions. In this study, we utilized ADSC-Exos in combination with GelMA hydrogel for wound treatment, and we observed a similar reduction in VEGF expression.

In this study, the Exos-GelMA composite hydrogel system employs a multi-target strategy for the prevention and treatment of HS and its efficacy was evaluated from two perspectives: collagen deposition and angiogenesis. However, further research is essential to analyze the mechanisms and long-term effects of exosomes. The causal relationship between the active components of exosomes, such as specific microRNAs and long non-coding RNAs, and their target genes has not been fully elucidated. Future research should focus on proteomic and transcriptomic profiling of exosome to elucidate the underlying antifibrotic and pro-regenerative mechanisms. The postoperative observation period was limited to 28 days, while the maturation period of human HS often extends to 6 to 12 months.[60,61] Therefore, extending the follow-up period to 12 weeks is necessary to adequately assess scar outcomes. In addition, future research also should include head-to-head comparisons with other common treatments and biomaterial strategies to benchmark the efficacy of Exos-GelMA hydrogel.

Conclusion

In summary, the Exos-GelMA composite hydrogel exhibits considerable prophylactic and therapeutic potential against HS in a rabbit ear HS model, which was restored collagen metabolic homeostasis and inhibited VEGF-mediated excessive neovascularization. These findings highlight its dual-action mechanism in modulating ECM remodeling and angiogenesis. This study confirms the Exos-GelMA as a novel injectable hydrogel system that integrates sustained-release Exosomes, presenting a promising cell-free therapy to alleviate HS.

Acknowledgments

Disclosure

The author(s) report no conflicts of interest in this work.

References

1. Xu X, Liu J, Xiao Z, et al. Zeolitic imidazolate framework-90 loaded with methylprednisolone sodium succinate effectively reduces hypertrophic scar in vivo. *Nanoscale*. 2024;16(13):6708–6719. doi:10.1039/D3NR05208G

2. Guo H, Guo Q, Ma Z. Kreotoxin A administration inhibits hyperproliferation and inflammation of human ear keloid tissue and keloid-derived fibroblasts by downregulating HIF-1α expression. *Biochem Biophys Res Commun*. 2024;715:149963. doi:10.1016/j.bbrc.2024.149963

3. Shen Y, Jin R, Liang X, et al. Angiogenesis modulation-mediated inhibitory effects of tacrolimus on hypertrophic scar formation. *Microvasc Res*. 2023;145:104446. doi:10.1016/j.mvr.2022.104446

4. Ogawa R. The most current algorithms for the treatment and prevention of hypertrophic scars and keloids: a 2020 update of the algorithms published 10 years ago. *Plast Reconstr Surg*. 2022;149(1):79e–94e. doi:10.1097/PRS.0000000000008667

5. Ogawa R, Dohi T, Tosa M, Aoki M, Akaishi S. The latest strategy for keloid and hypertrophic scar prevention and treatment: the nippon medical school (NMS. *Protocol J Nippon Med Sch*. 2021;88(1):2–9. doi:10.1272/jnms.JNMS.2021_88-106

6. Cho MY, Lee SG, Kim JE, Lee YS, Chang HS, Roh MR. Analysis of risk factors to predict occurrence and prognosis of postsurgical hypertrophic scar development: a review of 4238 cases. *Yonsei Med J*. 2023;64(11):687–691. doi:10.3349/ymj.2023.0003

7. Jin Z, Kim YS, Lim JY. Leveraging microneedles for raised scar management. *Polymers*. 2025;17(1):108. doi:10.3390/polym17010108

8. Knowles A, Glass DA. Keloids and hypertrophic scars. *Dermatol Clin*. 2023;41(3):509–517. doi:10.1016/j.det.2023.02.010

9. Xiong M, Yang X, Shi Z, et al. Programmable artificial skins accomplish antiscar healing with multiple appendage regeneration. *Adv Mater*. 2024;36(50):e2407322. doi:10.1002/adma.202407322

10. Zhang Z, Fan C, Xu Q, et al. A new strategy to inhibit scar formation by accelerating normal healing using silicate bioactive materials. *Adv Sci*. 2024;11(43):e2407718. doi:10.1002/advs.202407718

11. Abedanzadeh M, Abolmaali SS, Heidari R, et al. Photo-crosslinked hyaluronic acid hydrogels designed for simultaneous delivery of mesenchymal stem cells and tannic acid: advancing towards scarless wound healing. *Int J Biol Macromol*. 2024;281(Pt 4):136394. doi:10.1016/j.ijbiomac.2024.136394

12. Kohlhauser M, Mayrhofer M, Kamolz LP, Smolle C. An update on molecular mechanisms of scarring-a narrative review. *Int J mol Sci*. 2024;25(21):11579. doi:10.3390/ijms252111579

13. Gong X, Zhao Q, Zhang H, et al. The effects of mesenchymal stem cells-derived exosomes on metabolic reprogramming in scar formation and wound healing. *Int J Nanomed*. 2024;19:9871–9887. doi:10.2147/IJN.S480901

14. Li S, Li Y, Zhu K, et al. Exosomes from mesenchymal stem cells: potential applications in wound healing. *Life Sci*. 2024;357:123066. doi:10.1016/j.lfs.2024.123066

15. Hade MD, Suire CN, Suo Z. Mesenchymal stem cell-derived exosomes: applications in regenerative medicine. *Cells*. 2021;10(8):1959.

16. An Y, Lin S, Tan X, et al. Exosomes from adipose-derived stem cells and application to skin wound healing. *Cell Prolif*. 2021;54(3):e12993. doi:10.1111/cpr.12993

17. Zhou Y, Zhang XL, Lu ST, et al. Human adipose-derived mesenchymal stem cells-derived exosomes encapsulated in pluronic F127 hydrogel promote wound healing and regeneration. *Stem Cell Res Ther*. 2022;13(1):407. doi:10.1186/s13287-022-02980-3

18. Liang Q, Zhou D, Ge X, et al. Exosomes from adipose-derived mesenchymal stem cell improve diabetic wound healing and inhibit fibrosis via miR-128-1-5p/TGF-β1/Smad axis. *mol Cell Endocrinol*. 2024;588:112213. doi:10.1016/j.mce.2024.112213

19. Xu Z, Tian Y, Hao L. Exosomal miR-194 from adipose-derived stem cells impedes hypertrophic scar formation through targeting TGF-β1. *Mol Med Rep*. 2024;30(6):216. doi:10.3892/mmr.2024.13340

20. Ju Y, Hu Y, Yang P, Xie X, Fang B. Extracellular vesicle-loaded hydrogels for tissue repair and regeneration. *Mater Today Bio*. 2022;18:100522. doi:10.1016/j.mtbio.2022.100522

21. Lv B, Lu L, Hu L, et al. Recent advances in GelMA hydrogel transplantation for musculoskeletal disorders and related disease treatment. *Theranostics*. 2023;13(6):2015–2039. doi:10.7150/thno.80615

22. Xu W, Wang T, Wang Y, et al. An injectable platform of engineered cartilage gel and gelatin methacrylate to promote cartilage regeneration. *Front Bioeng Biotechnol*. 2022;10:884036. doi:10.3389/fbioe.2022.884036

23. AbadeDos Santos FA, Carvalho CL, Almeida I, et al. Simple method for establishing primary leporidae skin fibroblast cultures. *Cells*. 2021;10(8):2100. doi:10.3390/cells10082100

24. Zhou S, Wang Q, Yang W, et al. Development of a bioactive silk fibroin bilayer scaffold for wound healing and scar inhibition. *Int J Biol Macromol*. 2024;255:128350. doi:10.1016/j.ijbiomac.2023.128350

25. Dong Y, Wang H, Zhang Y, et al. NIR-II light based combinatorial management of hypertrophic scar by inducing autophagy in fibroblasts. *J Nanobiotechnol*. 2024;22(1):625. doi:10.1186/s12951-024-02876-9

26. Li S, Sun J, Yang J, et al. Gelatin methacryloyl (GelMA) loaded with concentrated hypoxic pretreated adipose-derived mesenchymal stem cells(ADSCs) conditioned medium promotes wound healing and vascular regeneration in aged skin. *Biomater Res*. 2023;27(1):11. doi:10.1186/s40824-023-00352-3

27. Grenier J, Duval H, Barou F, Lv P, David B, Letourneur D. Mechanisms of pore formation in hydrogel scaffolds textured by freeze-drying. *Acta Biomater*. 2019;94:195–203. doi:10.1016/j.actbio.2019.05.070

28. Mandal BB, Kundu SC. Cell proliferation and migration in silk fibroin 3D scaffolds. *Biomaterials*. 2009;30(15):2956–2965. doi:10.1016/j.biomaterials.2009.02.006

29. Cai SJ, Li CW, Weihs D, Wang GJ. Control of cell proliferation by a porous chitosan scaffold with multiple releasing capabilities. *Sci Technol Adv Mater*. 2017;18(1):987–996. doi:10.1080/14686996.2017.1406287

30. Loh QL, Choong C. Three-dimensional scaffolds for tissue engineering applications: role of porosity and pore size. *Tissue Eng Part B Rev*. 2013;19(6):485–502. doi:10.1089/ten.teb.2012.0437

31. Bružauskaitė I, Bironaitė D, Bagdonas E, Bernotienė E. Scaffolds and cells for tissue regeneration: different scaffold pore sizes-different cell effects. *Cytotechnology*. 2016;68(3):355–369. doi:10.1007/s10616-015-9895-4

32. Li Y, Sun Q, Hao L, et al. Liposomes loaded with 5-fluorouracil can improve the efficacy in pathological scars. *Int J Nanomed*. 2024;19:7353–7365. doi:10.2147/IJN.S466221

33. Goudarzi Afshar S, Tamri P, Nourian A, Moahmoudi A. Catechin hydrate improves hypertrophic scar in rabbit ear model via reduction of collagen synthesis. *Rep Biochem mol Biol*. 2024;13(1):13–22. doi:10.61186/rbmb.13.1.13

34. Shi J, Wu Y, Guo S, et al. The efficacy of anti-VEGF antibody-modified liposomes loaded with paeonol in the prevention and treatment of hypertrophic scars. *Drug Dev Ind Pharm*. 2019;45(3):439–455. doi:10.1080/03639045.2018.1546315

35. Frech FS, Hernandez L, Urbonas R, Zaken GA, Dreyfuss I, Nouri K. Hypertrophic scars and keloids: advances in treatment and review of established therapies. *Am J Clin Dermatol*. 2023;24(2):225–245. doi:10.1007/s40257-022-00744-6

36. Menchaca AD, Style CC, Olutoye OO. A review of hypertrophic scar and keloid treatment and prevention in the pediatric population: where are we now? *Adv Wound Care*. 2022;11(5):255–279. doi:10.1089/wound.2021.0028

37. Chen Q, Li S, Li K, Zhao W, Zhao C. A skin stress shielding platform based on body temperature-induced shrinking of hydrogel for promoting scar-less wound healing. *Adv Sci*. 2024;11(41):e2306018. doi:10.1002/advs.202306018

38. Zhang JJ, Li X, Tian Y, et al. Harnessing mechanical stress with viscoelastic biomaterials for periodontal ligament regeneration. *Adv Sci*. 2024;11(18):e2309562. doi:10.1002/advs.202309562

39. Hao S, Zhang Y, Meng J, et al. Integration of a superparamagnetic scaffold and magnetic field to enhance the wound-healing phenotype of fibroblasts [published correction appears in]. *ACS Appl Mater Inter*. 2019;11(3):3628. doi:10.1021/acsami.8b22375

40. Zhang T. Hepatocyte growth factor-modified adipose-derived mesenchymal stem cells inhibit human hypertrophic scar fibroblast activation. *J Cosmet Dermatol*. 2024;23(12):4268–4276. doi:10.1111/jocd.16509

41. Li S, Wang Y, Chen Y, Zhang H, Shen K, Guan H. PTEN hinders the formation of scars by regulating the levels of proteins in the extracellular matrix and promoting the apoptosis of dermal fibroblasts through Bcl-xL. *Arch Biochem Biophys*. 2024;753:109912. doi:10.1016/j.abb.2024.109912

42. Meng S, Wei Q, Chen S, et al. MiR-141-3p-functionalized exosomes loaded in dissolvable microneedle arrays for hypertrophic scar treatment. *Small*. 2024;20(8):e2305374. doi:10.1002/smll.202305374

43. Wu J, Song Y, Wang J, et al. Isorhamnetin inhibits hypertrophic scar formation through TGF-β1/Smad and TGF-β1/CREB3L1 signaling pathways. *Heliyon*. 2024;10(13):e33802. doi:10.1016/j.heliyon.2024.e33802

44. Cui J, Zhang S, Acharya K, et al. Decorin attenuates hypertrophic scar fibrosis via TGFβ/Smad signalling. *Exp Dermatol*. 2024;33(7):e15133. doi:10.1111/exd.15133

45. Tan Y, Zhang M, Kong Y, et al. Fibroblasts and endothelial cells interplay drives hypertrophic scar formation: insights from in vitro and in vivo models. *Bioeng Transl Med*. 2023;9(2):e10630. doi:10.1002/btm2.10630

46. Liu C, Tang L, Hou C, Zhang J, Li J. Intralesional axitinib injection mitigates hypertrophic scar by inhibiting angiogenesis pathway: a preliminary study in a rabbit ear model. *Clin Cosmet Invest Dermatol*. 2023;16:3023–3034. doi:10.2147/CCID.S430852

47. Yuan B, Upton Z, Leavesley D, Fan C, Wang XQ. Vascular and collagen target: a rational approach to hypertrophic scar management. *Adv Wound Care*. 2023;12(1):38–55. doi:10.1089/wound.2020.1348

48. Qi W, Zhuo M, Tian Y, Dawa Z, Bao J, An Y. Application of intelligent monitoring of percutaneous partial oxygen pressure in evaluating the evolution of scar hyperplasia. *J Healthc Eng*. 2023;2023:9781241. doi:10.1155/2023/9781241

49. Qi X, Liu Y, Yang M. Circ_0057452 functions as a ceRNA in hypertrophic scar fibroblast proliferation and VEGF expression by regulating TGF-β2 expression and adsorbing miR-145-5p. *Am J Transl Res*. 2021;13(6):6200–6210.

50. Zhou N, Li D, Luo Y, Li J, Wang Y. Effects of botulinum toxin type a on microvessels in hypertrophic scar models on rabbit ears. *Biomed Res Int*. 2020;2020:2170750. doi:10.1155/2020/2170750

51. Cheng L, Sun X, Hu C, et al. In vivo early intervention and the therapeutic effects of 20(s)-ginsenoside rg3 on hypertrophic scar formation. *PLoS One*. 2014;9(12):e113640. doi:10.1371/journal.pone.0113640

52. Li C, Wei S, Xu Q, Sun Y, Ning X, Wang Z. Application of ADSCs and their exosomes in scar prevention. *Stem Cell Rev Rep*. 2022;18(3):952–967. doi:10.1007/s12015-021-10252-5

53. Xiang H, Ding P, Qian J, et al. Exosomes derived from minor salivary gland mesenchymal stem cells: a promising novel exosome exhibiting pro-angiogenic and wound healing effects similar to those of adipose-derived stem cell exosomes. *Stem Cell Res Ther*. 2024;15(1):462. doi:10.1186/s13287-024-04069-5

54. Xu C, Zhang H, Yang C, et al. miR-125b-5p delivered by adipose-derived stem cell exosomes alleviates hypertrophic scarring by suppressing Smad2. *Burns Trauma*. 2024;12:tkad064. doi:10.1093/burnst/tkad064

55. Li Y, Zhang J, Shi J, et al. Exosomes derived from human adipose mesenchymal stem cells attenuate hypertrophic scar fibrosis by miR-192-5p/IL-17RA/Smad axis [published correction appears in]. *Stem Cell Res Ther*. 2021;12(1):490. doi:10.1186/s13287-021-02568-3

56. Li J, Yin Y, Zou J, et al. The adipose-derived stem cell peptide ADSCP2 alleviates hypertrophic scar fibrosis via binding with pyruvate carboxylase and remodeling the metabolic landscape. *Acta Physiol*. 2023;238(4):e14010. doi:10.1111/apha.14010

57. Wang M, Zhao J, Li J, Meng M, Zhu M. Insights into the role of adipose-derived stem cells and secretome: potential biology and clinical applications in hypertrophic scarring. *Stem Cell Res Ther*. 2024;15(1):137. doi:10.1186/s13287-024-03749-6

58. Li Y, Xiao Y, Shang Y, et al. Exosomes derived from adipose tissue-derived stem cells alleviated H_2O_2-induced oxidative stress and endothelial-to-mesenchymal transition in human umbilical vein endothelial cells by inhibition of the mir-486-3p/Sirt6/Smad signaling pathway. *Cell Biol Toxicol*. 2024;40(1):39. doi:10.1007/s10565-024-09881-6

59. Higginbotham S, Workman VL, Giblin AV, Green NH, Lambert DW, Hearnden V. Inhibition and reversal of a TGF-β1 induced myofibroblast phenotype by adipose tissue-derived paracrine factors. *Stem Cell Res Ther.* 2024;15(1):166. doi:10.1186/s13287-024-03776-3

60. Bharadia SK, Burnett L, Gabriel V. Hypertrophic scar. *Phys Med Rehabil Clin N Am.* 2023;34(4):783–798. doi:10.1016/j.pmr.2023.05.002

61. Edwards J. Hypertrophic scar management. *Br J Nurs.* 2022;31(20):S24–S31. doi:10.12968/bjon.2022.31.20.S24